RSC Pharmaceutics

ROYAL SOCIETY OF CHEMISTRY

PAPER

View Article Online
View Journal | View Issue

Cite this: *RSC Pharm.*, 2026, **3**, 574

Fucoidan/bis-MPA-based dendrimer nanoparticles with intrinsic anti-angiogenic activity for oncology applications

Filipe Olim,[a] Ana Duarte,[a] Ana Rute Neves,[a] Irene Rodriguez-Clemente,[b] Joel T. Kidgell,[c] Barbara C. Wimmer,[c] Valentín Ceña [b] and Helena Tomás *[a]

Nanoparticles with intrinsic anti-angiogenic activity hold strong promise in cancer nanomedicine, as they can both help suppress metastasis and deliver therapeutics, offering a dual strategy for addressing the disease. In this study, fucoidans from *F. vesiculosus* and *U. pinnatifida* with two different molecular weights (M_W) of each were initially screened for *in vitro* anti-angiogenic potential using the tube formation assay with HUVEC cells. The higher M_W fucoidans, which represent native M_W fucoidan, exhibited greater anti-angiogenic activity and were subsequently combined with 2,2-bis(hydroxymethyl)propionic acid (bis-MPA)-based dendrimers (generation 2) at different fucoidan/dendrimer (F/D) mass ratios to form self-assembled nanoparticles through electrostatic interactions. Optimisation yielded two nanoparticle types with positive (F/D = 1 : 2) and negative (F/D = 2 : 1) zeta potentials, which were characterised for their physicochemical properties, including hydrodynamic diameter, zeta potential, chemical composition (FTIR), and morphology (TEM). These nanoparticles presented a near-spherical shape, were cytocompatible, and did not cause haemolysis. Positively charged nanoparticles showed stronger anti-angiogenic activity than negatively charged ones. Since the dendrimers alone were also anti-angiogenic, the overall effect likely results from the combined contribution of both components, with nanoparticle assembly potentially playing a role. Overall, these findings highlight the potential of fucoidan/dendrimer nanoparticles as multifunctional platforms for cancer nanomedicine, by targeting angiogenesis and potentially serving as drug or gene delivery systems.

Received 2nd December 2025,
Accepted 6th February 2026

DOI: 10.1039/d5pm00362h

rsc.li/RSCPharma

Introduction

Angiogenesis, the process of forming new blood vessels from existing ones, plays a critical role in the growth and progression of malignant tumours.[1,2] By facilitating the supply of oxygen and nutrients, angiogenesis supports the development of solid tumours and provides a pathway for tumour cells to spread throughout the body, leading to metastasis. Recognizing the importance of angiogenesis in cancer therapy, researchers have explored the use of angiogenesis blockade therapy.[3,4] However, these angiogenesis blockade agents face challenges such as limited efficacy, the occurrence of treatment resistance, and significant adverse effects.[5] Consequently, the search for new anti-angiogenic molecules continues, alongside investigations into innovative administration techniques that hold promise for more effective cancer therapies.

Nanomedicine offers diverse approaches for addressing angiogenesis in tumours.[6] Firstly, nanomaterials can serve as drug delivery systems, not only transporting cytostatic anticancer drugs but also carrying angiogenesis blockade agents. Due to the abnormal and more permeable nature of newly formed vessels in tumours, along with insufficient lymphatic drainage, these nanomaterials tend to accumulate within the tumour site. This phenomenon, known as the enhanced permeability and retention (EPR) effect, enables passive targeting of the tumour. Alternatively, nanomaterials can be specifically designed to actively target biological receptors by functionalizing their surfaces with chemical groups or biomolecules, such as antibodies. This affinity of a nanomaterial for a receptor can be used as an anti-angiogenesis strategy too, as pro-angiogenic factors (like VEGF) or their correspondent receptors can be inactivated in this way. In fact, one expects that the combination of passive and active targeting will result in an enhanced delivery and action of therapeutic agents concomitantly with fewer side effects for the patient.

Fucoidan, a remarkable molecule, can be extracted from the cell walls of various species of brown seaweeds.[7,8] Native fucoidan is an anionic, polydisperse, and high-molecular-

[a]*CQM-Centro de Química da Madeira, MMRG, Universidade da Madeira, Campus da Penteada, 9020-105 Funchal, Portugal. E-mail: lenat@staff.uma.pt*
[b]*Unidad Asociada Neurodeath, School of Medicine, University of Castilla-La Mancha, 02006 Albacete, Spain*
[c]*Marinova Pty Ltd, 249 Kennedy Drive, Cambridge, TAS 7170, Australia*

weight polysaccharide that may present varying degrees of sulfation, differences in constituent sugar composition, peak molecular weight (M_W) and degree of branching. While its backbone primarily consists of the deoxy monosaccharide L-fucose, it also encompasses several other sugars like galactose, xylose, mannose, arabinose, and rhamnose. The backbone itself is formed by glycosidic bonds that may be α(1 → 3) or alternating α(1 → 3) and α(1 → 4). The composition, M_W, and structure of fucoidan are influenced by a multitude of factors, including the source species and developmental stage of the seaweed, its habitat, and the extraction method employed. This complexity adds to the versatility of fucoidan, which has been shown to exhibit an array of important biological activities, including anticoagulant, antiviral, immunomodulatory, antioxidant, and anti-inflammatory properties.[8–10] Fucoidan has also demonstrated potential as a cancer-fighting agent through multiple mechanisms, such as triggering cell apoptosis, enhancing the immune system's ability to eliminate cancer cells, and inhibiting cell migration.[7,11–13] Moreover, fucoidan from different origins, compositions, and molecular weights have been linked to an anti-angiogenic effect that may further contribute to an anti-metastatic action.[14–17] However, in this respect, it should be noted that not all studies are in agreement, as some suggest that fucoidan may also have an opposite effect.[18–20] Therefore, selecting the appropriate fucoidan – considering its source species, M_W, and extraction technique – is crucial for achieving the desired biological activity. In fact, it is believed that the anti- or pro-angiogenic properties of fucoidan may vary depending on its M_W, composition (namely, the sulfation degree), and structure.[7]

Given the fucoidans' bioactivities and the advantages of nanomedicine approaches in cancer therapy, several types of nanomaterials containing fucoidan or fucoidan derivatives in their composition have been developed.[7,21] For this purpose, different experimental strategies have been used, such as self-assembly, microwave-assisted, emulsion and solvent evaporation, green synthesis, precipitation, and ultrasonication methods.[22,23] Mostly, these fucoidan-based nanomaterials are hybrid structures, incorporating other polymers and/or inorganic materials, and were designed to be applied not only as drug delivery systems but also for diagnostic purposes such as serving as contrast agents in medical imaging.[23–25] Importantly, fucoidan exhibits notable affinity for P-selectin, a protein highly expressed in tumour vasculature and thus may confer tumour targetability to nanoparticles,[26] particularly to sites of active angiogenesis. In addition, there is emerging evidence suggesting that fucoidan may have the ability to facilitate the crossing of the blood-brain barrier which is also related with its interaction with P-selectin present in stimulated endothelial cells.[27] In fact, the advantages linked to fucoidan-based nanoparticles keep encouraging research in the field. In this scope, the combination of fucoidan with cationic polymers, including natural and synthetic polycations (like chitosan, protamine, and polyethyleneimine), was particularly explored.[7,21] The main reason behind this option is that nanoparticles can be easily formed solely driven by the electrostatic attractions established between the opposite charged polymers in a self-assembly process.

Dendrimers are nanoscale polymers, featuring a central core, branching units, and terminal functional groups.[28] With each addition of monomer layers to the central core, the dendrimer increases in generation. Due to the possibility of precisely controlling their size, shape, and surface functionalities, dendrimers show tuneable properties and have been applied in the biomedical field as drugs *per se*, as controlled drug delivery/theranostic systems (alone or combined with other chemical entities), and as components in biosensors.[28–33] Among their possible chemical composition, the dendrimers based on the 2,2-bis(hydroxymethyl)propionic acid (bis-MPA dendrimers) monomer are notable for their biodegradability into non-toxic products which makes them particularly attractive for use in the biomedical field.[34–38] These dendrimers can be synthesized with various terminal groups, including hydroxyl, carboxyl, and ammonium groups, making them highly adaptable for use and integration with other building blocks in the fabrication of hybrid nanomaterials.

The objective of this work was to evaluate the possibility of preparing nanoparticles based on fucoidan and bis-MPA dendrimers, simply using a self-assembly process (Fig. 1), aimed at being used in nanomedicine as possible drug delivery systems with intrinsic anti-angiogenic activity. First, preliminary experiments based on *in vitro* tube formation by endothelial cells (HUVEC cells) were performed to evaluate the anti-angiogenic properties of fucoidan itself from two different species – the algae *Fucus vesiculosus* and *Undaria pinnatifida* –, as the source can impact fucoidan's chemical composition and structure. Moreover, experiments were carried out with fucoidans fractionated to lower M_w under controlled conditions, enabling the analysis of the impact of molecular weight on anti-angiogenic activity. The best fucoidan candidates in terms of anti-angiogenic activity were then combined with generation 2 bis-MPA dendrimers at different fucoidan/

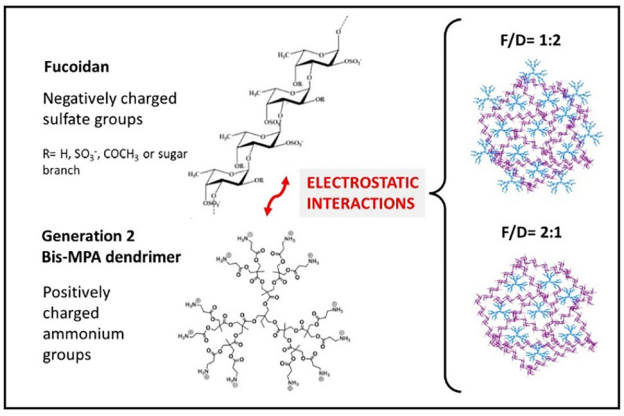

Fig. 1 Scheme of hybrid fucoidan/dendrimer nanoparticle preparation solely based on electrostatic interactions. Fucoidan was combined with generation 2 bis-MPA dendrimers at two different fucoidan/dendrimer (F/D) mass ratios to obtain self-assembled nanoparticles (a general structure of fucoidan is shown).

dendrimer (F/D) mass ratios to obtain self-assembled nanoparticles. These hybrid fucoidan/dendrimer nanoparticles were characterized with respect to their physicochemical properties, as well as their cytocompatibility, anti-angiogenic activity, and hemocompatibility, including effects on haemolysis and coagulation, with a view toward their future application as drug or gene delivery systems.

Results and discussion

Fucoidan: chemical characterization, cytotoxicity and *in vitro* anti-angiogenic activity

The present study used fucoidan from *Fucus vesiculosus* and *Undaria pinnatifida* extracted by a proprietary aqueous extraction process by Marinova Pty Ltd (Tasmania, Australia) and stored at ambient temperature (21–29 °C). Fucoidan was used both in its extracted form (native M_w) and after undergoing an additional fractionation process, which isolated lower M_w molecules. Table 1 summarizes the chemical composition and molecular weight of the four types of fucoidan used: native molecular weight and fractionated fucoidan from *F. vesiculosus* (FVF and FVF-F, respectively) and native molecular weight and fractionated fucoidan from *U. pinnatifida* (UPF and UPF-F, respectively). It is possible to observe that fucoidan from *F. vesiculosus* has a higher total carbohydrate content when compared to fucoidan from *U. pinnatifida*. It also has a slightly higher content of uronic acid, and a slightly lower degree of sulfation compared to that of *U. pinnatifida*. However, the most distinctive features of these two types of fucoidan lie in their carbohydrate profiles. In this regard, the fucoidan derived from *F. vesiculosus* is notably rich in fucose, whereas that extracted from *U. pinnatifida* stands out for its high galactose content. This characteristic was not significantly affected by the fractionation process, although slight variations were observed in the content of less abundant carbohydrates within the original polysaccharides. Peak molecular weight of native fucoidan for *F. vesiculosus* fucoidan was 51.1 kDa and for fractionated fucoidan it was 20.7 kDa; and from *U. pinnatifida* fucoidan it was 84.3 kDa and 8.2 kDa, respectively.

The anti-angiogenic activity of the four fucoidan types was evaluated *in vitro* using human umbilical vein endothelial cells (HUVEC cells) which are primary cells derived from the endothelium of umbilical cord veins and often used as a cell model to investigate the molecular mechanisms underlying blood vessel formation. Prior to these studies, fucoidan cytotoxicity was studied using a metabolic activity assay that relies on the reduction of resazurin. This method provides an indirect assessment of cell viability as viable cells use mitochondrial and other cellular reductases to convert resazurin into the fluorescent compound resorufin that can be measured by fluorescence spectroscopy. Fig. 2 presents the results for the different fucoidans across the 10–1000 μg mL^{-1} concentration range after 24 h of cell culture. The data are expressed as a percentage of the metabolic activity observed in the control, which consisted of cells incubated solely in cell culture medium. The results indicate that fucoidan, regardless of its source or M_w, does not significantly affect cell viability within the tested concentration interval. This information enabled the use of the same concentration range for studying the effect of fucoidan on the angiogenesis process, as the results will not be affected by cell death. Indeed, the information available in the literature shows that the cytotoxicity of fucoidan depends significantly not only on its intrinsic characteristics but also on the type of cells used in the experiments, highlighting the importance of conducting this evaluation on a case-by-case basis.[39]

Subsequently, the anti-angiogenic effect of various forms of fucoidan was assessed *in vitro* using the tube formation assay, a test that evaluates the ability of endothelial cells to form capillary-like structures on a 3D extracellular matrix, mimick-

Table 1 Peak molecular weight (M_W) and composition of the fucoidan used in the experiments

	F. vesiculosus		*U. pinnatifida*	
	FVF	FVF-F	UPF	UPF-F
Composition (% of dry weight)				
Total carbohydrates	67.5	71.5	64	61.3
Uronic acid	2.0	2.2	0.9	0.7
Polyphenol	<2	<2	<2	<2
Sulfate	26	26.9	31	27.6
Cations	11.2	8.8	6.8	6.0
Peak M_W (kDa)	51.1	20.7	84.3	8.2
Carbohydrate profile (mol%)				
Fucose	**89.9**	**77.6**	**50.4**	**67.3**
Xylose	3.9	6.1	4.0	0
Mannose	0.7	2.1	0	0.7
Galactose	3.8	5.4	**45.6**	**30.5**
Glucose	0.4	7.2	0	0.8
Arabinose	0.7	0.5	0	0
Rhamnose	0.5	1.1	0	0.6

FVF = native fucoidan from *F. vesiculosus*; FVF-F = fractionated fucoidan from *F. vesiculosus*; UPF = native fucoidan from *U. pinnatifida*; UPF-F = fractionated fucoidan from *U. pinnatifida*.

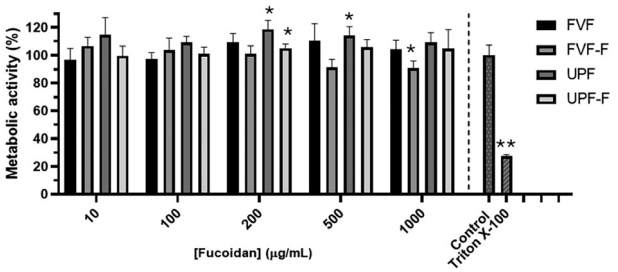

Fig. 2 Effect of fucoidan concentration on the metabolic activity of HUVEC cells after 24 h (FVF = native fucoidan from *F. vesiculosus*; FVF-F = fractionated fucoidan from *F. vesiculosus*; UPF = native fucoidan from *U. pinnatifida*; UPF-F = fractionated fucoidan from *U. pinnatifida*). Results are expressed as a percentage of the negative control (only cell culture medium); medium containing Triton-X was used as positive control. Data represents the mean ± SD (n = 4, *p < 0.05, **p < 0.001 as compared to the control).

ing the initial stages of angiogenesis.[40] For this, HUVEC cells were seeded on a pre-solidified gel and treated with the four fucoidan polysaccharides. After 6 h of incubation, live cells were stained, tube formation was observed under a fluorescence microscope, and several parameters indicative of the angiogenic process were quantified based on the obtained images. The results shown in Fig. 3 clearly demonstrate that incomplete tube formation occurs when fucoidan is added to the cell culture medium. The extent of this effect depends on both the dose applied and the type of fucoidan used. Indeed, an anti-angiogenic effect is already observed at a fucoidan concentration of 100 μg mL^{-1}, with this effect becoming significantly more pronounced at higher concentrations (500 and 1000 μg mL^{-1}). Not only do the images obtained reflect this effect from a qualitative point of view, but it is also supported by the quantitative data, namely vessel area, number of junctions, and lacunarity (Fig. 4). Regarding the total area covered by the capillary-like structures formed by the endothelial cells on the extracellular matrix (vessel area), one can see that it decreases with concentration for all fucoidan types when compared with the control (in the absence of fucoidan). In the case

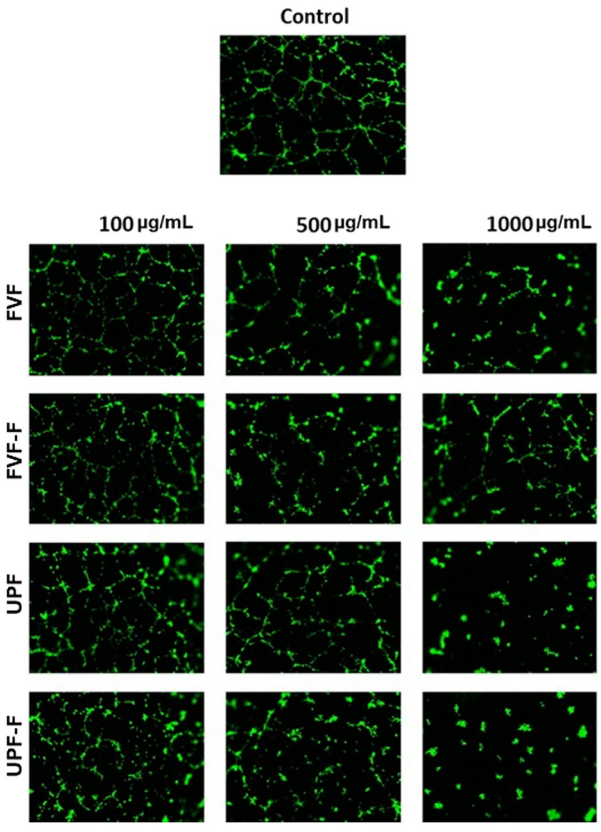

Fig. 3 Fluorescence microscopy images representative of calcein-AM-labeled tubes formed by HUVEC cells after 6 h of exposure to 100, 500 or 1000 μg mL^{-1} of the four types of fucoidan (FVF = native fucoidan from *F. vesiculosus*; FVF-F = fractionated fucoidan from *F. vesiculosus*; UPF = native fucoidan from *U. pinnatifida*; UPF-F = fractionated fucoidan from *U. pinnatifida*). The control refers to cells in the gel matrix incubated only in cell culture medium. All images are at a 40× magnification.

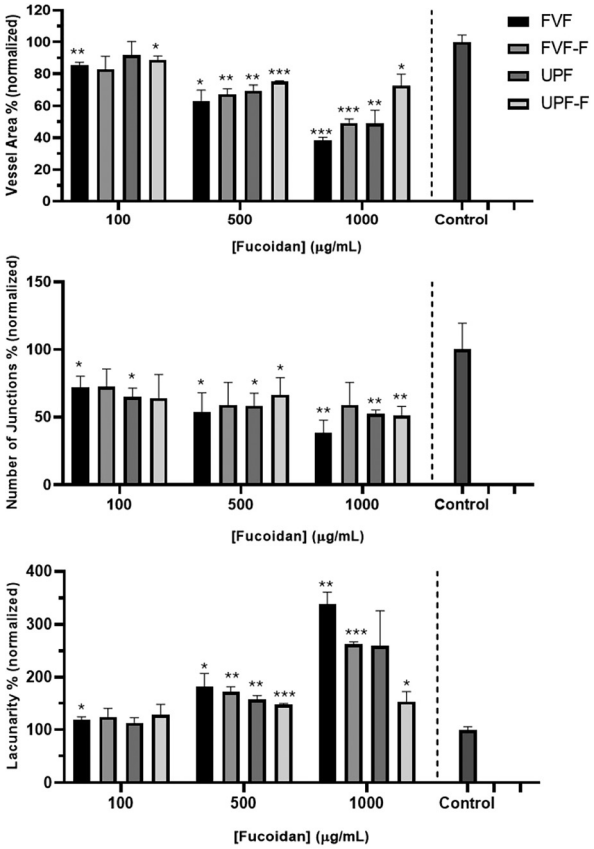

Fig. 4 Vessel area, number of junctions, and lacunarity calculated based on images from the tube formation assay. HUVEC cells were exposed to 100, 500 or 1000 μg mL^{-1} of the four types of fucoidan (FVF = native fucoidan from *F. vesiculosus*; FVF-F = fractionated fucoidan from *F. vesiculosus*; UPF = native fucoidan from *U. pinnatifida*; UPF-F = fractionated fucoidan from *U. pinnatifida*). The control refers to cells in the gel matrix incubated only in cell culture medium. Data represents the mean ± SD (n = 3, *p < 0.05, **p < 0.01, ***p < 0.001 as compared to the control).

of junctions, which represent points where multiple tubular structures intersect, representing the branching complexity of the network, the results also show a clear pattern of inhibition in the presence of fucoidan. In addition, an increase in the network's irregularity and fragmentation as fucoidan concentration rises is observed, which is reflected in higher lacunarity values. This indicates more disordered structures, which are consistent with an anti-angiogenic effect too.

When analysing the results, the observed anti-angiogenic effect differs depending on whether the fucoidan is derived from *F. vesiculosus* or *U. pinnatifida*, as well as whether the polysaccharide is the native extract or an isolated low M_w fraction. For the fucoidan from *F. vesiculosus*, the best anti-angiogenic effect was observed with the native polymer (FVF, peak M_w 51.1 kDa). For fractionated fucoidan (FVF-F, peak M_w 20.7 kDa), angiogenesis inhibition was not so pronounced. The fractionated form of fucoidan from *U. pinnatifida* (UPF-F, peak M_w 8.2 kDa), in turn, exhibited the weakest anti-angiogenic effect among the four types of fucoidan tested, while its

native form (UPF, peak M_w 84.3 kDa) displayed a behaviour very similar to that of fractionated fucoidan from *F. vesiculosus*. Overall, it can be concluded that, on the one hand, lower M_w fractions of fucoidan reduces the anti-angiogenic effect, while, on the other hand, the fucoidan from *F. vesiculosus* had a superior anti-angiogenic effect compared to that from *U. pinnatifida.* The distinct monosaccharide composition of fucoidan from *F. vesiculosus* – including its higher fucose and lower galactose content – along with its lower sulfate and higher cation levels, may alone or collectively contribute to the observed effect. The highly branched structure of fucoidan from *U. pinnatifida*[41] may also contribute to a lower anti-angiogenic activity.

In vivo angiogenesis involves complex interactions between endothelial cells, signalling molecules, and the surrounding tissue environment. It requires the coordinated action of multiple signalling molecules, which promote endothelial cell proliferation, migration, and tube formation. Additionally, angiogenesis involves not only vessel growth but also remodelling and stabilization, where pro-angiogenic factors are balanced by anti-angiogenic signals to ensure proper vascular development. As expected, *in vitro* angiogenesis, such as in the tube formation assay, only mimics some aspects of the angiogenic process, being a simplified version. This assay is, however, very useful as a model for studying early-stage angiogenesis and testing potential interfering compounds. Fibroblast growth factor (FGF) and epidermal growth factor (EGF), factors that promote angiogenesis, are present in the cell culture medium where HUVEC cells are cultured. HUVEC cells will then produce other pro-angiogenic factors, such as VEGF and angiopoietins, that work together, initiating and regulating the formation of new blood vessels. Indeed, VEGF is known to upregulate angiopoietin-2 (Ang-2) production in HUVEC cells, especially during the early stages of angiogenesis. With this in mind, Ang-2 expression was measured as a possible angiogenesis-related marker to further assess the effect of the four types of fucoidan in the *in vitro* tube formation assay. Results are shown in Fig. 5 and are in line with previous findings. Although no significant differences are observed among all samples at a fucoidan concentration of 100 μg mL^{-1}, at a fucoidan concentration of 1000 μg mL^{-1} in the media, a concentration at which more marked differences are expected to be observed, Ang-2 levels in the cell culture supernatants collected at the end of the tube formation assay were lower for native fucoidan derived from *F. vesiculosus* (FVF), suggesting a stronger anti-angiogenic action. Also, fractionated fucoidan from *U. pinnatifida* (UPF-F) led to values that were not significantly different from the control, seeming to be the less potent inhibitor of angiogenesis. The other two fucoidan types (FVF-F and UPF) presented intermediate Ang-2 expression values which are not significantly different from each other.

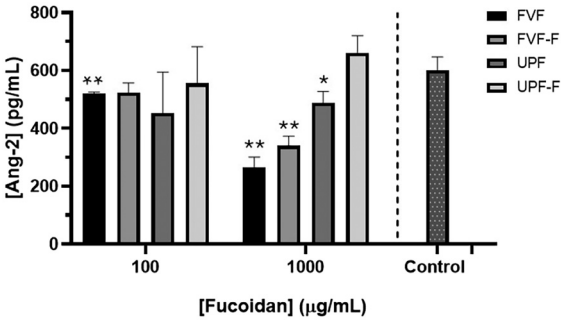

Fig. 5 Expression of angiopoietin-2 (Ang-2) measured in cell supernatants obtained in the tube formation assay. HUVEC cells were exposed to 100 or 1000 μg mL^{-1} of the four types of fucoidan (FVF = native fucoidan from *F. vesiculosus*; FVF-F = fractionated fucoidan from *F. vesiculosus*; UPF = native fucoidan from *U. pinnatifida*; UPF-F = fractionated fucoidan from *U. pinnatifida*). The control refers to cells in the gel matrix incubated only in cell culture medium. Data represents the mean ± SD (n = 3, *p < 0.05, **p < 0.01 as compared to the control).

Fucoidan/bis-MPA-based dendrimer nanoparticles: preparation and physicochemical characterization

For the preparation of fucoidan/bis-MPA-based dendrimer nanoparticles, native fucoidan from *F. vesiculosus* (FVF) and *U. pinnatifida* (UPF) were selected due to their higher anti-angiogenic potential compared to their fractionated counterparts. Nanoparticle preparation was based on a simple self-assembly process driven by the electrostatic interactions between two oppositely charged polymers: the negatively charged fucoidan, which contains sulfate groups along its structure, and the positively charged generation 2 bis-MPA dendrimer, which has protonated amine groups at its periphery. The experimental procedure involved mixing an aqueous fucoidan solution to an aqueous dendrimer solution at room temperature at different fucoidan/dendrimer (F/D) mass ratios.

Following an optimization process, two types of nanoparticles were consistently obtained based on F/D mass ratios of 1 : 2 and 2 : 1. Table 2 presents the hydrodynamic diameter and the zeta potential values measured for the nanoparticles prepared at these ratios with fucoidan from *F. vesiculosus* (FVF 1 : 2 and FVF 2 : 1) and *U. pinnatifida* (UPF 1 : 2 and UPF 2 : 1). Whereas nanoparticles with an F/D ratio of 1 : 2 exhibit a positive zeta potential, those with an F/D ratio of 2 : 1 exhibit a negative one, regardless of the type of fucoidan used. This is due to the balance between positive and negative charges in the nanoparticles. Specifically, a positive zeta potential reflects a higher number of dendrimers present and greater exposure of protonated amine groups on the nanoparticle surface, while

Table 2 Hydrodynamic diameter, polydispersity and zeta potential of nanoparticles prepared at different fucoidan/dendrimer ratios (FVF = native fucoidan from F. vesiculosus; UPF = native fucoidan from U. pinnatifida). Data represents the mean (n = 3), relative standard deviations were <10%, and the polydispersity index (PDI) was always <0.2

Nanoparticle	Hydrodynamic diameter (nm) *Z*-Average	PDI	Zeta potential (mV)
FVF 1 : 2	166	0.08	+32
FVF 2 : 1	113	0.18	−32
UPF 1 : 2	176	0.14	+25
UPF 2 : 1	160	0.14	−42

a negative zeta potential indicates a higher amount of fucoidan and greater exposure of its sulfate groups. Importantly, the absolute values of zeta potential are very high which is an indicator of colloidal stability. High absolute zeta potential values (positive or negative) will lead to strong repulsion between the nanoparticles and prevent their aggregation, preserving their properties and functionality over time. This is a crucial aspect considering that the fucoidan/dendrimer nanoparticles are expected to be used in cancer treatment, possibly as gene/drug delivery systems, taking advantage of their intrinsic anti-angiogenic properties. Additionally, for the F/D ratio of 1 : 2, nanoparticles prepared with fucoidan extracted from *F. vesiculosus* exhibit a significantly more positive zeta potential than those based on fucoidan from *U. pinnatifida*. Consistently, for the 2 : 1 ratio, this value is less negative.

The *Z*-average, also known as the cumulants mean, is a commonly used parameter in dynamic light scattering (DLS) measurements, representing the intensity-weighted harmonic mean of the particle size distribution. This parameter is meaningful primarily for monodisperse or nearly monodisperse samples. In this study, it was considered equivalent to the hydrodynamic diameter, as the polydispersity index (PDI) was <0.2 for all formulations, indicating that the nanoparticle populations were relatively homogeneous in terms of size. The hydrodynamic diameter of the fucoidan/dendrimer nanoparticles ranged from 113 to 176 nm, with nanoparticles prepared at an F/D ratio of 1 : 2 exhibiting higher values than those prepared at an F/D ratio of 2 : 1. Positive nanoparticles (with a higher content in dendrimers) thus seemed to be less compacted in solution than the negative ones. Interestingly, nanoparticles prepared with fucoidan from *F. vesiculosus* were smaller than those made with fucoidan from *U. pinnatifida* which may be related with the fact that fucoidan from *U. pinnatifida* tends to be more branched. When analysing the fucoidan/dendrimer nanoparticles by transmission electron microscopy (Fig. 6), information was also gathered regarding morphology. The nanoparticles were found to adopt a near-spherical shape and appeared dehydrated, with some looking collapsed. Their size was similar to that measured in aqueous solution (in some cases smaller, as expected), but no significant differences could be seen among the samples.

Fourier-transform infrared spectroscopy (FTIR) was used to further characterize the fucoidan/dendrimer nanoparticles, confirming the presence of both fucoidan and dendrimers within their structure. Fig. 7 shows the spectra of the nanoparticles based on fucoidan from *F. vesiculosus* and from *U. pinnatifida* at the F/D ratios of 1 : 2 and 2 : 1. The figure also contains the spectra from the individual starting polymers that can be compared with those arising from the nanoparticles (more detailed information regarding FTIR spectra analysis is presented in the SI, Fig. S1–S7 and Tables S1–S3). The dendrimer alone exhibits a spectrum with highly intense absorption bands. In the spectra of the nanoparticles, the bands corresponding to the dendrimers are clearly visible and can even mask those of fucoidan. Interestingly, the spectra of nanoparticles prepared at an F/D ratio of 1 : 2, whether with fucoidan from *F. vesiculosus* or *U. pinnatifida*, show very intense absorption bands associated with the dendrimers (the spectra are largely superimposable), reflecting a high dendrimer content in these nanoparticles. Conversely, in the spectra of nanoparticles prepared at an F/D ratio of 2 : 1, as expected, the dendrimer-related bands are significantly less intense. Nevertheless, undoubtedly, the presence of fucoidan in the nanoparticles is confirmed by the characteristic band at ≈1220 cm^{-1} due to S=O asymmetric stretching vibration. The broad band in the range of 3200–3600 cm^{-1}, corresponding to O–H stretching vibrations, is also very strong, but the contribution of water molecules in this spectral region must also be taken into account.

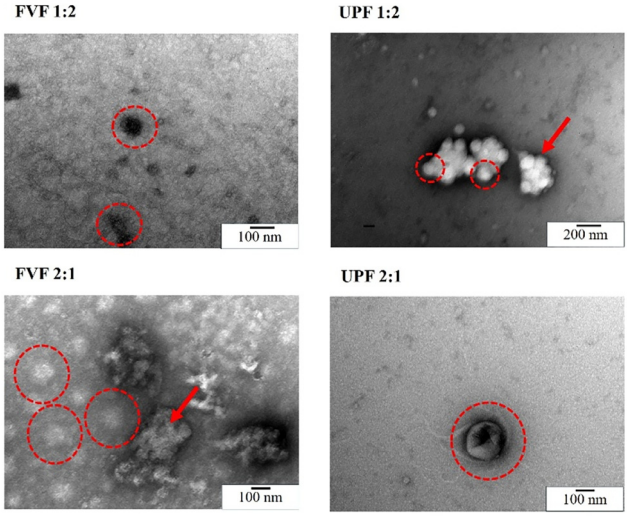

Fig. 6 Transmission electron microscope images of the fucoidan/dendrimer nanoparticles at the two F/D ratios (1 : 2 and 2 : 1) after negative staining using uranyl acetate (FVF = native fucoidan from *F. vesiculosus*; UPF = native fucoidan from *U. pinnatifida*). The red arrow is pointing to agglomerates.

Fucoidan/bis-MPA-based dendrimer nanoparticles: anti-angiogenic activity and blood compatibility

Studies were further conducted on the cytotoxicity and anti-angiogenic potential of fucoidan/dendrimer nanoparticles. Like previously, nanoparticles were prepared with FVF (native fucoidan from *F. vesiculosus*) or UPF (native fucoidan from *U. pinnatifida*) at F/D ratios of 1 : 2 or 2 : 1, and their concentration was expressed based on their fucoidan content for consistency and comparability. In relation to the studies using fucoidan alone, these experiments were conducted at lower fucoidan concentrations, in the range 10 to 50 μg mL^{-1}, more aligned with the range of concentration expected to be present in the target tumour tissues – it is known that, on average, only ~0.7% of the injected nanoparticle dose effectively accumulates in solid tumours.[42] Indeed, while initial plasma concentrations may be in the microgram range after intravenous injection, biological barriers (*e.g.*, clearance by the reticu-

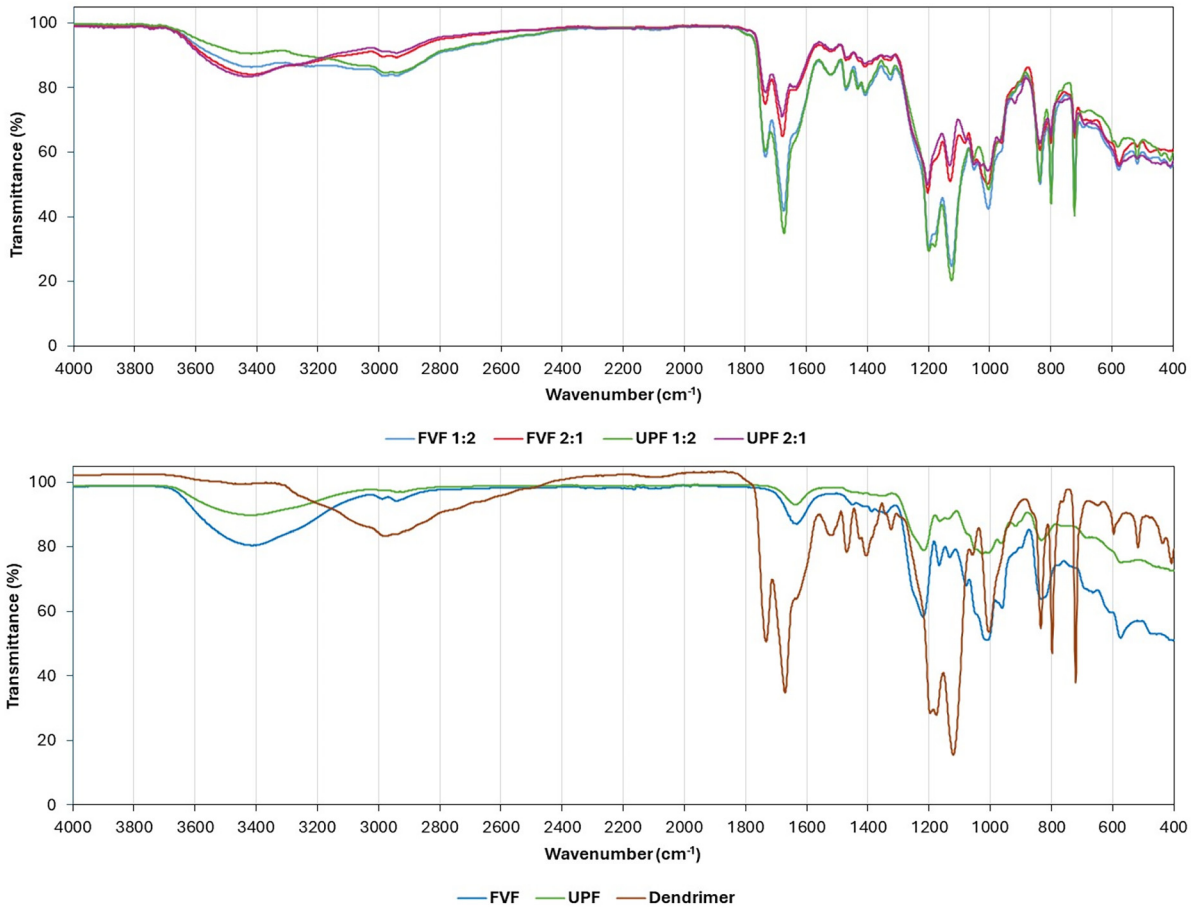

Fig. 7 FTIR spectra for the fucoidan/dendrimer nanoparticles prepared with FVF (native fucoidan from *F. vesiculosus*) or UPF (native fucoidan from *U. pinnatifida*) at F/D ratios of 1 : 2 or 2 : 1 (top image); FTIR spectra for native fucoidans and for the bis-MPA dendrimer (bottom image).

loendothelial system, limited tumour penetration) significantly reduce the amount that reaches the tumour site.[28]

Fig. 8 shows the effect of the concentration of fucoidan/dendrimer nanoparticles on the metabolic activity of HUVEC cells after 24 h exposure. As expected, the results indicate that none of the nanoparticle types tested were cytotoxic within the concentration range studied as metabolic activity was not significantly different from the control. The fact that the nanoparticles do not affect cell viability is likely due to both fucoidan and bis-MPA dendrimers being non-cytotoxic at the concentrations used (see Fig. S8 in SI, which shows the effect of dendrimer concentration on the metabolic activity of HUVEC cells).

Again, the tube formation assay was used, this time to evaluate whether the nanoparticles retained the anti-angiogenic activity observed with fucoidan alone. Interestingly, the nanoparticles exhibited anti-angiogenic activity, despite the lower fucoidan content in the culture medium. Although this effect is less apparent by simple observation of fluorescence microscopy images after cell staining (Fig. 9), quantitative analysis of these images reveals that the tube network formed by HUVEC cells is less developed (with less vessel area, fewer junctions, and higher lacunarity) (Fig. 10). This effect was significantly more pronounced in nanoparticles prepared with F/D ratios of 1 : 2, regardless of the type of fucoidan used (from *F. vesiculosus* or *U. pinnatifida*). These results suggested that bis-MPA dendrimers could contribute to the anti-angiogenic effect observed in the nanoparticles. To explore this, the

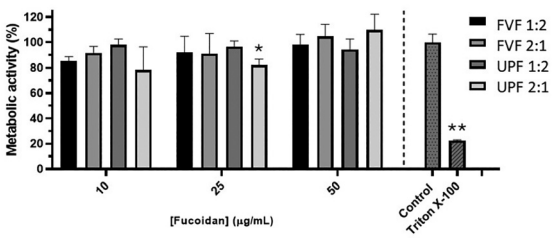

Fig. 8 Effect of the concentration of fucoidan/dendrimer nanoparticles on the metabolic activity of HUVEC cells after 24 h (nanoparticle concentration is expressed based on the fucoidan content). Nanoparticles were prepared with FVF (native fucoidan from *F. vesiculosus*) or UPF (native fucoidan from *U. pinnatifida*) at F/D ratios of 1 : 2 or 2 : 1. Results are expressed as a percentage of the negative control (only cell culture medium); medium containing Triton-X was used as positive control. Data represents the mean ± SD (n = 3, *p < 0.05, **p < 0.001 as compared to the control).

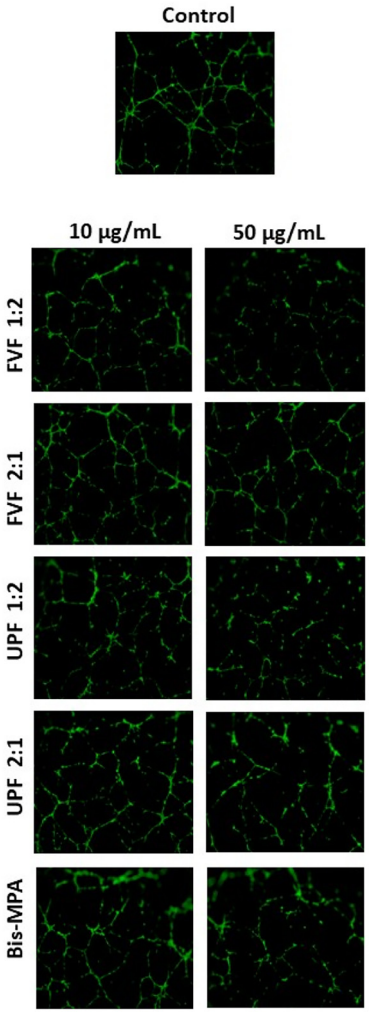

Fig. 9 Fluorescence microscopy images representative of calcein-AM-labeled tubes formed by HUVEC cells after 6 h of exposure to nanoparticles at 10 and 50 μg mL^{-1} (nanoparticle concentration is expressed based on the fucoidan content), and to dendrimers alone at corresponding concentration values. Nanoparticles were prepared with FVF (native fucoidan from *F. vesiculosus*) or UPF (native fucoidan from *U. pinnatifida*) at F/D ratios of 1 : 2 or 2 : 1. The control refers to cells in the gel matrix incubated only in cell culture medium. All images are at a 40× magnification.

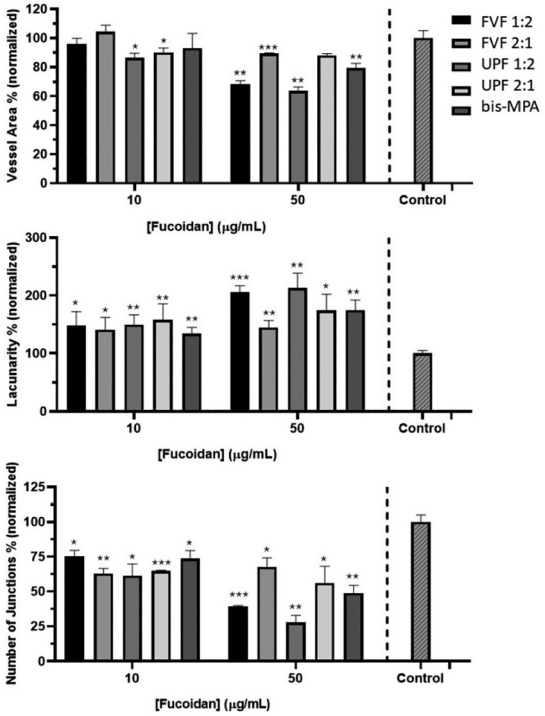

Fig. 10 Vessel area, number of junctions, and lacunarity calculated based on images from the tube formation assay. HUVEC cells were exposed to nanoparticles at 10 and 50 μg mL^{-1} (nanoparticle concentration is expressed based on the fucoidan content), and to dendrimers alone at corresponding concentration values. Nanoparticles were prepared with FVF (native fucoidan from *F. vesiculosus*) or UPF (native fucoidan from *U. pinnatifida*) at F/D ratios of 1 : 2 or 2 : 1. The control refers to cells in the gel matrix incubated only in cell culture medium. Data represents the mean ± SD (n = 3, *p < 0.05, **p < 0.01, ***p < 0.001 as compared to the control).

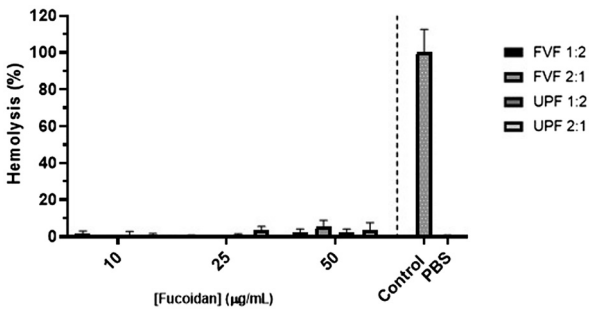

Fig. 11 Effect of fucoidan/dendrimer nanoparticle concentration on human erythrocyte haemolysis (nanoparticle concentration is expressed based on the fucoidan content). Nanoparticles were prepared with FVF (native fucoidan from *F. vesiculosus*) or UPF (native fucoidan from *U. pinnatifida*) at F/D ratios of 1 : 2 or 2 : 1. Results are expressed as the percentage of haemolysis relative to the water-treated blood (control), which represents 100% haemolysis Data represents the mean ± SD (n = 4, p < 0.001 as compared to the control in all cases).

effect of the dendrimers alone was also investigated, and it was found that they also exerted a significant anti-angiogenic effect (Fig. 10). Therefore, the anti-angiogenic properties of fucoidan/dendrimer nanoparticles are likely due to a combined effect of both fucoidan and the dendrimers, while the role of nanoparticle assembly itself cannot be excluded.

Blood compatibility is a key parameter to evaluate when assessing nanoparticles intended for intravenous use, as is the case in the present study. To investigate this, the impact of fucoidan/dendrimer nanoparticles on human erythrocyte haemolysis was first analysed. As shown in Fig. 11, the extent of haemolysis did not differ significantly from the control (DPBS without calcium and magnesium) thus indicating that the fucoidan/dendrimer nanoparticles are well-tolerated by these cells. Furthermore, assessing the potential impact of nanoparticles on the coagulation system is also critical to ensure

their safe use in this context. The coagulation assay was conducted using a pool of human plasma with calcium chloride serving as the clotting initiator. The progression of clot formation was monitored by measuring absorbance at 405 nm over time, allowing for real-time tracking of the coagulation process. Clotting times were determined by identifying the time point at which the absorbance curve reaches a plateau, indicating the completion of fibrin network formation. Fig. 12 presents the results obtained in a representative experiment. Of the four types of nanoparticles tested, those prepared from fucoidan derived from *F. vesiculosus* (FVF 1 : 2 and FVF 2 : 1) and from *U. pinnatifida* at an F/D ratio of 1 : 2 followed the trend of the reference control, showing no interference in the clotting process. In contrast, the UPF 2 : 1 nanoparticles significantly reduced clotting time by approximately 20 minutes. This result was unexpected as the literature consistently indicates that fucoidan extracted from *U. pinnatifida* exhibits anticoagulant – not procoagulant – properties.[43] However, in nanoparticles, fucoidan is presented in a highly dense manner on the surface, which may enhance its interactions with plasma proteins, and coagulation factors, possibly creating a procoagulant microenvironment that differs from free fucoidan in solution. Possibly, this pro-coagulant effect is due to the high negative zeta potential shown by the UPF 2 : 1 fucoidan/dendrimer nanoparticles (−42 mV). In fact, it is known that the intrinsic coagulation pathway is initiated by negatively charged surfaces.[44,45] Interestingly, a study involving carboxyl-modified polystyrene nanoparticles with a hydrodynamic diameter of 220 nm and a zeta potential of −43.5 mV showed that they were able to initiate the intrinsic pathway of coagulation, whereas smaller particles having a hydrodynamic diameter of 24 nm and a zeta potential of −49.2 mV were unable to do it.[46] This observation may account for the lack of procoagulant activity in FVF 2 : 1 fucoidan/dendrimer nanoparticles, which, despite their negative zeta potential (−32 mV), are considerably smaller (113 nm). The differences in M_W, branching and composition between fucoidan of *F. vesiculosus* and *U. pinnatifida* thus conduct to nanoparticles with distinct physicochemical properties and different interaction with blood components.

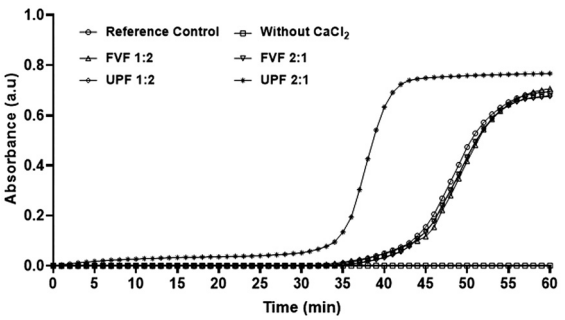

Fig. 12 Effect of fucoidan/dendrimer nanoparticle concentration on human blood coagulation time (nanoparticle concentration was 50 μg mL^{-1} expressed on the fucoidan content). Nanoparticles were prepared with FVF (native fucoidan from *F. vesiculosus*) or UPF (native fucoidan from *U. pinnatifida*) at F/D ratios of 1 : 2 or 2 : 1. Controls were done without $CaCl_2$ (the clotting initiator) and with NaCl 0.9% (w/v) (the reference). The image is representative of 3 independent experiments.

Conclusions

This work demonstrated that the native fucoidans from *F. vesiculosus* and *U. pinnatifida* possess a superior anti-angiogenic activity *in vitro* compared to fucoidans from the same species fractionated to lower molecular weights. Also, the compositional differences in the fucoidans from different species of seaweed may have contributed to their bioactivity. When combined with generation 2 bis-MPA-based dendrimers at varying mass ratios, the fucoidans with higher M_W formed self-assembled nanoparticles through electrostatic interactions. Optimisation experiments led to the development of two nanoparticle types with distinct zeta potentials (positive at F/D = 1 : 2 and negative at F/D = 2 : 1), which were shown to contain both fucoidan and dendrimers, to be of a near spherical shape, and to have anti-angiogenic properties *in vitro* – positively charged nanoparticles (F/D 1 : 2) consistently showed a stronger inhibition of tube formation than negatively charged ones. The anti-angiogenic activity observed for the fucoidan/dendrimer nanoparticles was likely driven by both components, but a potential contribution from the self-assembled structure could not be excluded. Importantly, the nanoparticles were cytocompatible and did not induce haemolysis or blood coagulation, except for the UPF 2 : 1 nanoparticles. Overall, these findings provide preliminary *in vitro* evidence supporting the potential of fucoidan/dendrimer nanoparticles as multifunctional platforms for cancer nanomedicine, combining anti-angiogenic activity with the possibility of future drug or gene delivery applications. Further evaluation in more advanced models, including *in vivo* studies, will be important to confirm these findings, together with dedicated stability studies to assess the long-term physicochemical behaviour of the nanoparticles over time. Also, mechanistic studies investigating the signalling pathways underlying the anti-angiogenic effects will be important future work to further consolidate the findings of the present study.

Author contributions

All authors contributed to this study. F. Olim performed most of the experimental work.

Conflicts of interest

Joel Kidgell and Barbara C. Wimmer are employed by Marinova Pty. Ltd, and the other authors declare that there are no potential conflicts of interest. Marinova Pty. Ltd had no role in the study design, collection, analysis, interpretation of data, the writing of this article or the decision to submit it for publication.

Ethical statement

Human blood used in the haemocompatibility studies was provided by the Funchal Central Hospital in accordance with the guidelines and approval of the Hospital's Ethics Committee. Written informed consent was obtained from all donors prior to sample collection. Donor data were fully anonymized. Only residual blood samples from routine clinical analyses were used; no additional blood was collected specifically for the purposes of this study.

Data availability

The data supporting this article are included either in the main text or as part of the supplementary information (SI). Supplementary information: experimental methods, and additional figures. See DOI: https://doi.org/10.1039/d5pm00362h.

Acknowledgements

This work was supported by FCT – *Fundação para a Ciência e a Tecnologia* through national funds as part of the project Centro de Química da Madeira, UID/00674/2025 (https://doi.org/10.54499/UID/00674/2025). F. O. acknowledges ARDITI-Agência Regional para o Desenvolvimento da Investigação Tecnologia e Inovação for the Ph.D. fellowship M1420-09-5369-FSE-000002. V. C. thanks the support of MCIN and JCCM with funding from European Union NextGenerationEU (PRTR-C17.I1); by MINECO/AEI/FEDER/UE (MCIN/AEI/10.13039/501100011033) project PID2024-161254OB-I00, and by University of Castilla-La Mancha project 2022-GRIN-34370.

References

1 S. Rosińska and J. Gavard, *Int. J. Mol. Sci.*, 2021, **22**, 6514.
2 R. Lugano, M. Ramachandran and A. Dimberg, *Cell. Mol. Life Sci.*, 2020, **77**, 1745–1770.
3 M. J. Ansari, D. Bokov, A. Markov, A. T. Jalil, M. N. Shalaby, W. Suksatan, S. Chupradit, H. S. Al-Ghamdi, N. Shomali, A. Zamani, A. Mohammadi and M. Dadashpour, *Cell Commun. Signaling*, 2022, **20**, 49.
4 B. Yetkin-Arik, A. W. Kastelein, I. Klaassen, C. H. J. R. Jansen, Y. P. Latul, M. Vittori, A. Biri, K. Kahraman, A. W. Griffioen, F. Amant, C. A. R. Lok, R. O. Schlingemann and C. J. F. van Noorden, *Biochim. Biophys. Acta, Rev. Cancer*, 2021, **1875**, 188446.
5 Y. Haibe, M. Kreidieh, H. E. Hajj, I. Khalifeh, D. Mukherji, S. Temraz and A. Shamseddine, *Front. Oncol.*, 2020, **10**, 221.
6 H. O. Alsaab, A. S. Al-Hibs, R. Alzhrani, K. K. Alrabighi, A. Alqathama, A. Alwithenani, A. H. Almalki and Y. S. Althobaiti, *Int. J. Mol. Sci.*, 2021, **22**, 1631.
7 S. M. Etman, Y. S. R. Elnaggar and O. Y. Abdallah, *Int. J. Biol. Macromol.*, 2020, **147**, 799–808.
8 J. Fitton, D. Stringer and S. Karpiniec, *Mar. Drugs*, 2015, **13**, 5920–5946.
9 J. H. Fitton, A. Y. Park, S. S. Karpiniec and D. N. Stringer, *Mar. Drugs*, 2020, **19**, 4.
10 J. H. Fitton, D. N. Stringer, A. Y. Park and S. S. Karpiniec, *Mar. Drugs*, 2019, **17**, 571.
11 X. He, M. Xue, S. Jiang, W. Li, J. Yu and S. Xiang, *Biol. Pharm. Bull.*, 2019, **42**, 442–447.
12 X. Chen, L. Sun, X. Wei, H. Lu, Y. Tan, Z. Sun and J. Jiang, *BMC Complementary Med. Ther.*, 2021, **21**, 25.
13 E. Turrini, F. Maffei and C. Fimognari, *Mar. Drugs*, 2023, **21**, 307.
14 F. Liu, J. Wang, A. K. Chang, B. Liu, L. Yang, Q. Li, P. Wang and X. Zou, *Phytomedicine*, 2012, **19**, 797–803.
15 Q. Cong, H. Chen, W. Liao, F. Xiao, P. Wang, Y. Qin, Q. Dong and K. Ding, *Carbohydr. Polym.*, 2016, **136**, 899–907.
16 C. Oliveira, N. M. Neves, R. L. Reis, A. Martins and T. H. Silva, *Carbohydr. Polym.*, 2020, **239**, 116131.
17 J. Ohmes, Y. Xiao, F. Wang, M. D. Mikkelsen, T. T. Nguyen, H. Schmidt, A. Seekamp, A. S. Meyer and S. Fuchs, *Mar. Drugs*, 2020, **18**, 481.
18 N. E. Ustyuzhanina, M. I. Bilan, N. A. Ushakova, A. I. Usov, M. V. Kiselevskiy and N. E. Nifantiev, *Glycobiology*, 2014, **24**, 1265–1274.
19 W. Wen, L. Yang, X. Wang, H. Zhang, F. Wu, K. Xu, S. Chen and Z. Liao, *Int. Wounds*, 2023, **20**, 3606–3618.
20 C. Bouvard, I. Galy-Fauroux, F. Grelac, W. Carpentier, A. Lokajczyk, S. Gandrille, S. Colliec-Jouault, A. M. Fischer and D. Helley, *Mar. Drugs*, 2015, **13**, 7446–7462.
21 P. H. L. Tran, W. Duan and T. T. D. Tran, *Int. J. Pharm.*, 2020, **575**, 118956.
22 J. Venkatesan, S. S. Murugan and G. H. Seong, *Int. J. Biol. Macromol.*, 2022, **217**, 652–667.
23 R. J. B. Pinto, D. Bispo, C. Vilela, A. M. P. Botas, R. A. S. Ferreira, A. C. Menezes, F. Campos, H. Oliveira, M. H. Abreu, S. A. O. Santos and C. S. R. Freire, *Materials*, 2020, **13**, 1076.
24 J. Gonçalves, C. Nunes, L. Ferreira, M. M. Cruz, H. Oliveira, V. Bastos, Á. Mayoral, Q. Zhang and P. Ferreira, *Nanomaterials*, 2021, **11**, 2939.
25 Y. Chen, J. Wang, Q. Wang, X. Lei, J. Zhao, Z. Xu and J. Ming, *ACS Sustainable Chem. Eng.*, 2023, **11**, 11745–11755.
26 Y. Shamay, M. Elkabets, H. Li, J. Shah, S. Brook, F. Wang, K. Adler, E. Baut, M. Scaltriti, P. V. Jena, E. E. Gardner, J. T. Poirier, C. M. Rudin, J. Baselga, A. Haimovitz-Friedman and D. A. Heller, *Sci. Transl. Med.*, 2016, **8**, 345ra87.
27 D. E. Tylawsky, H. Kiguchi, J. Vaynshteyn, J. Gerwin, J. Shah, T. Islam, J. A. Boyer, D. R. Boué, M. Snuderl, M. B. Greenblatt, Y. Shamay, G. P. Raju and D. A. Heller, *Nat. Mater.*, 2023, **22**, 391–399.
28 H. Tomás and J. Rodrigues, in *New Trends in Smart Nanostructured Biomaterials in Health Sciences*, Elsevier, 2023, pp. 41–78.

29 S. Mignani, X. Shi, V. Ceña, J. Rodrigues, H. Tomás and J.-P. Majoral, *J. Controlled Release*, 2021, **332**, 346–366.
30 D. Maciel, C. Guerrero-Beltrán, R. Ceña-Diez, H. Tomás, M. Á Muñoz-Fernández and J. Rodrigues, *Nanoscale*, 2019, **11**, 9679–9690.
31 I. Martins, H. Tomás, F. Lahoz and J. Rodrigues, *Biomacromolecules*, 2021, **22**, 2436–2450.
32 C. Camacho, H. Tomás and J. Rodrigues, *Molecules*, 2021, **26**, 2924.
33 M. Urbanowicz, K. Sadowska, B. Lemieszek, A. Paziewska-Nowak, A. Sołdatowska, M. Dawgul and D. G. Pijanowska, *Bioelectrochemistry*, 2023, **152**, 108407.
34 A. Carlmark, E. Malmström and M. Malkoch, *Chem. Soc. Rev.*, 2013, **42**, 5858.
35 S. García-Gallego, A. M. Nyström and M. Malkoch, *Prog. Polym. Sci.*, 2015, **48**, 85–110.
36 M. Gonçalves, V. Kairys, J. Rodrigues and H. Tomás, *Biomacromolecules*, 2022, **23**, 20–33.
37 P. Stenström, D. Manzanares, Y. Zhang, V. Ceña and M. Malkoch, *Molecules*, 2018, **23**, 2028.
38 N. Feliu, M. V. Walter, M. I. Montañez, A. Kunzmann, A. Hult, A. Nyström, M. Malkoch and B. Fadeel, *Biomaterials*, 2012, **33**, 1970–1981.
39 K. S. Bittkau, P. Dörschmann, M. Blümel, D. Tasdemir, J. Roider, A. Klettner and S. Alban, *Mar. Drugs*, 2019, **17**, 441.
40 Y. Kubota, H. K. Kleinman, G. R. Martin and T. J. Lawley, *J. Cell Biol.*, 1988, **107**, 1589–1598.
41 H. T. T. Cao, M. D. Mikkelsen, M. J. Lezyk, L. M. Bui, V. T. T. Tran, A. S. Silchenko, M. I. Kusaykin, T. D. Pham, B. H. Truong, J. Holck and A. S. Meyer, *Mar. Drugs*, 2018, **16**, 422.
42 S. Wilhelm, A. J. Tavares, Q. Dai, S. Ohta, J. Audet, H. F. Dvorak and W. C. W. Chan, *Nat. Rev. Mater.*, 2016, **1**, 1–12.
43 Y. Qi, L. Wang, Y. You, X. Sun, C. Wen, Y. Fu and S. Song, *Foods*, 2022, **11**, 822.
44 C. Naudin, E. Burillo, S. Blankenberg, L. Butler and T. Renné, *Semin. Thromb. Hemostasis*, 2017, **43**, 814–826.
45 S. Park and J. K. Park, *Blood Res.*, 2024, **59**, 35.
46 C. Oslakovic, T. Cedervall, S. Linse and B. Dahlbäck, *Nanomedicine*, 2012, **8**, 981–986.